



# The ligand polyhedral model: some further considerations of tetrahedral clusters with 12 carbonyl ligands

Brian F.G. Johnson\*, Steven Tay

University Chemical Laboratory, Lensfield Road, Cambridge CB2 1EW, UK

Received 16 January 2003; received in revised form 7 March 2003; accepted 20 March 2003

Dedicated to Professor Renato Ugo on the occasion of his 65th birthday

## Abstract

The molecular structures of a series of tetrahedral clusters containing the central  $[M_4(CO)_{12}]$  unit have been examined in the light of the ligand polyhedral model. Within this series fall the three anionic clusters  $[Rh_3Ru(CO)_{12}]^-$ ,  $[Rh_3Os(CO)_{12}]^-$  and  $[Rh_2Ru_2(CO)_{12}]^{2-}$ . These are unusual in that the carbonyl polyhedron does not conform to the icosahedron  $\{12\}$  (symmetry  $I$ ), the cubeoctahedron or the *anti*-cubeoctahedron usually observed but instead are based on the *nido*-capped icosahedron  $\{13-1\}$ . The complete series exhibits a transformation from icosahedron ( $C_{3v}$  molecular structure adopted for  $[Co_4(CO)_{12}]$ ) to the *nido*-capped icosahedron ( $C_s$  molecular symmetry adopted for  $[Rh_3Os(CO)_{12}]^-$ ) according to the approach adopted by Dunitz and Burgi. These observations represent an extension of the LPM along the lines previously reported in our consideration of the polyhedral growth sequence in which each successive polyhedron with vertices from 4 to 12 is generated first by edge-cleavage and then a capping operation. However, it is clear that the presence of anionic charge and/or the presence of counter cation(s) plays a dominant role in the final adopted carbonyl arrangement and polyhedral form.

© 2003 Elsevier Science B.V. All rights reserved.

**Keywords:** Ligand polyhedral model; Polyhedral growth sequence; Carbonyls; Clusters; Structure

## 1. Introduction

The ligand polyhedral model (LPM), first proposed in 1976, was based on ideas derived from a consideration of polyhedral geometries and was applied to a wide range of binary carbonyls [1]. For 12-ligand clusters, three main ligand polytopes were identified: the icosahedron, the cubeoctahedron and the *anti*-cubeoctahedron. As explained by the LPM, the icosahedron is the most common geometry observed due to its stability while the cubeoctahedron and *anti*-

cubeoctahedron were adopted only when the metal core size was large [1]. However, recent synthetic and X-ray diffraction studies of the  $[Rh_3Ru(CO)_{12}]^-$ ,  $[Rh_3Os(CO)_{12}]^-$  and  $[Rh_2Ru_2(CO)_{12}]^{2-}$  anionic clusters present a ligand polytope that deviates significantly from the icosahedron and cannot be identified as any known *ideal* polyhedra [2–4]. These structures differ from other similar 12-carbonyl anionic clusters in that they possess two carbonyl ligands which bridge the basal–apical metal–metal bond. Here, we wish to propose a system of classification which allows us to incorporate these structures into the LPM employing the concept of the *nido*-polyhedral ligand arrangement. This idea originates from the simple relationship between polyhedra in which each

\* Corresponding author. Tel.: +44-1223-336-337;  
fax: +44-1223-336017.  
E-mail address: [bfgj1@cam.ac.uk](mailto:bfgj1@cam.ac.uk) (B.F.G. Johnson).

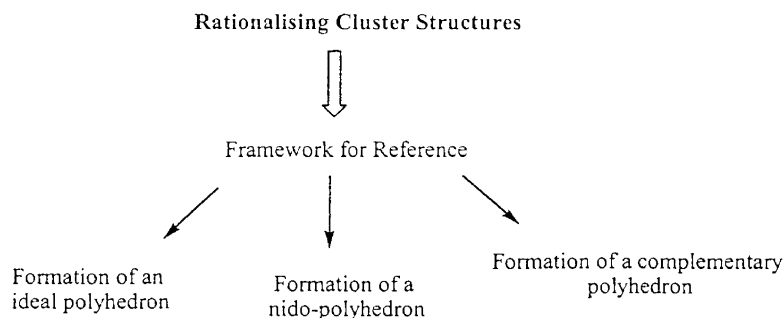


Fig. 1. The LPM as a framework for rationalising cluster structures.

successive polyhedron may be produced from its immediate predecessor by the process of edge-cleavage followed by a capping process and which we have discussed in detail elsewhere [5]. Hence, structures produced before the capping process (ideal polyhedra with one or more vertices missing) may be considered as stable and in agreement with this view have been observed in both simple co-ordination complexes and cluster compounds. A good example is the square-based pyramid which corresponds to a *nido*-octahedron {6–1}. This clearly illustrates the role of the LPM as a framework for rationalising cluster structures (Fig. 1), although the reasons for the variation in the form adopted remains unclear.

## 2. Results and discussion

In many five-coordinate compounds, both the trigonal bipyramidal {5} and square-based pyramidal {6–1} geometries may be observed. This is best illustrated by the crystal structure of  $[\text{Cr}(\text{en})_3][\text{Ni}(\text{CN})_5]$ , where the  $[\text{Ni}(\text{CN})_5]^{3-}$  anion is found in both these geometric forms in the same crystal. Here, the square-based pyramid may be considered as a *nido*-octahedron {6–1} (Fig. 2).

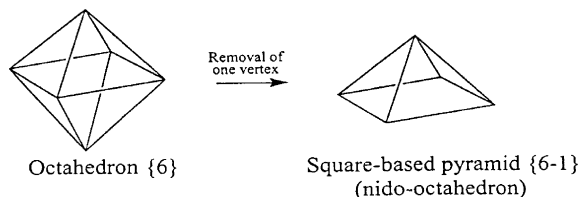


Fig. 2. The formation of a *nido*-octahedron.

Such *nido* structures are moderately common and in several transition metal clusters ligand shells describing a *nido*-polyhedron have been observed. For example,  $[\text{Fe}_3(\text{CO})_{11}]^{2-}$  [6], has a *nido*-icosahedral ligand envelope {12–1} (Fig. 3). Here, removal of one vertex from the parent icosahedron presents an ‘open’ pentagonal face.

In contrast, but totally as expected,  $[\text{Ru}_3(\text{CO})_{11}]^{2-}$  may be described as containing a *nido*-(anti-cubeoctahedral) ligand envelope but which shows a significant distortion towards the *nido*-icosahedral form<sup>1</sup> (Figs. 4 and 5) [7].

Although the crystal structure of the osmium analogue,  $[\text{Os}_3(\text{CO})_{11}]^{2-}$ , is not available, the similarity of its IR spectrum in the CO region to that of  $[\text{Ru}_3(\text{CO})_{11}]^{2-}$  indicates that it possesses the same structure [8].

The molecular structure of  $[\text{Rh}_4(\text{CO})_{12}]$  [9] more or less describes an icosahedron (*see below*) and as a consequence the  $[\text{Rh}_4(\text{CO})_{11}]^{2-}$  dianion might be expected to have a *nido*-icosahedral ligand envelope similar to that of  $[\text{Fe}_3(\text{CO})_{11}]^{2-}$ . Surprisingly, it describes the alternative but unusual *nido*- $D_{3h}$  icosahedron (Fig. 6) [10].

This  $D_{3h}$  icosahedron despite being a fully triangulated polyhedron, has three vertices with a connectivity of four (A), six vertices with connectivity of five (B) and three vertices with a connectivity of six (C) (Fig. 7). The removal of a type A vertex results in an ‘open’ square face. This corresponds to the most stable *nido*- $D_{3h}$  icosahedral form as it maximises the remaining inter-ligand interactions. Removal of a type

<sup>1</sup> A similar slight distortion is shown by the parent molecule  $[\text{Ru}_3(\text{CO})_{12}]$ .

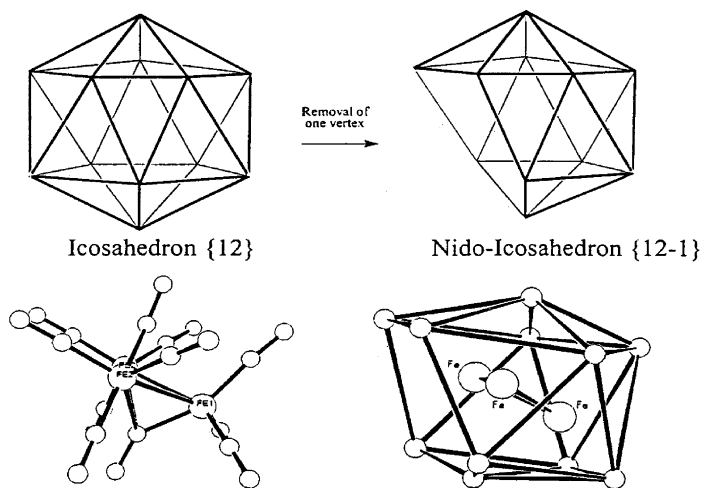


Fig. 3. The *nido*-icosahedral ligand polytope of  $[\text{Fe}_3(\text{CO})_{11}]^{2-}$ .

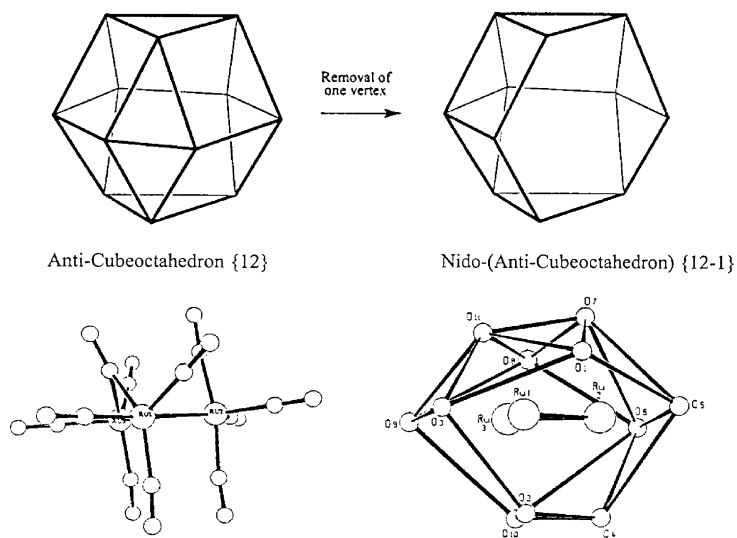


Fig. 4. The *nido*-(anti-cubeoctahedral) ligand polytope  $[\text{Ru}_3(\text{CO})_{11}]^{2-}$ .

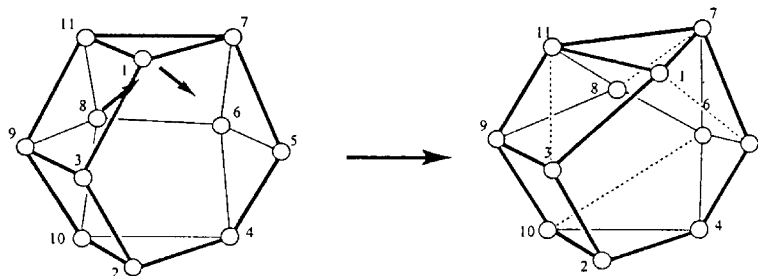


Fig. 5. Proposed distortion mode of the *nido*-(anti-cubeoctahedron).

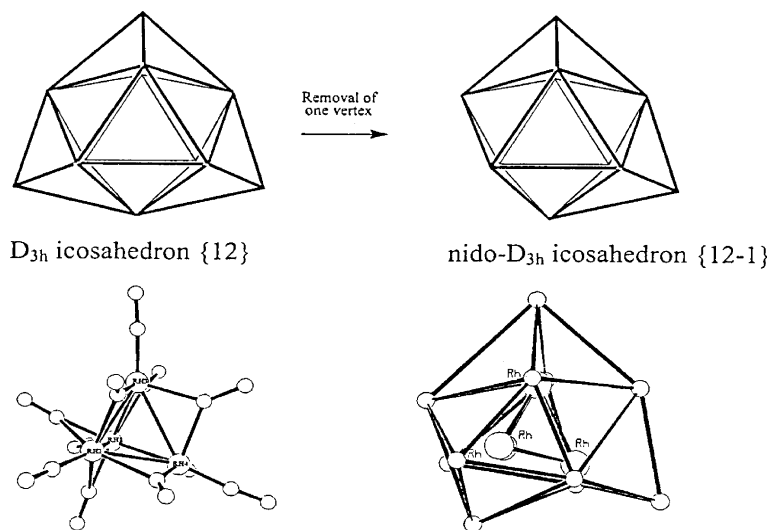


Fig. 6. The *nido*- $D_{3h}$  icosahedral ligand polytope of  $[\text{Rh}_4(\text{CO})_{11}]^{2-}$ .

B or a type C ligand results in an ‘open’ pentagonal or hexagonal face, respectively. These two *nido*- $D_{3h}$  icosahedral forms may be regarded as being of higher energy (i.e. less stable) than that derived by removal of an A type vertex.

The observation that the  $[\text{Rh}_4(\text{CO})_{11}]^{2-}$  adopts this *nido*- $D_{3h}$  icosahedral form rather than the *nido*-icosahedral (symmetry I) form reflects the relative ease of conversion between the I-icosahedral and  $D_{3h}$ -icosahedral geometries (i.e. energetically close polyhedra) which has been discussed elsewhere.

In contrast, in the three anions  $[\text{Rh}_3\text{Ru}(\text{CO})_{12}]^-$ ,  $[\text{Rh}_3\text{Os}(\text{CO})_{12}]^-$  and  $[\text{Rh}_2\text{Ru}_2(\text{CO})_{12}]^{2-}$ , the distorted icosahedral ligand shells observed are similar to the *nido*-(1:5:6:1) polyhedron. This is formed from the 13-vertex (1:5:6:1) polyhedron—formed by the edge-cleavage addition process from the icosahedron—

the faced-capped icosahedron by the removal of one vertex (see Fig. 8).

The specific vertex removed to form the *nido*-(1:5:6:1) polyhedron has a connectivity of three and its removal leads to a polyhedron with an ‘open’ face of six vertices describing a ‘chair’ conformation (Fig. 9a). The similarity of this polyhedron and the distorted icosahedron in  $[\text{Rh}_3\text{Ru}(\text{CO})_{12}]^-$ ,  $[\text{Rh}_3\text{Os}(\text{CO})_{12}]^-$  and  $[\text{Rh}_2\text{Ru}_2(\text{CO})_{12}]^{2-}$  (Fig. 9b) is clear and can be readily shown from two points of view. First, the Föppl notation is 1:5:5:1 with a vertex clearly missing from the second hexagonal plane (Fig. 9c). Second, there is an ‘open’ face of six vertices which describes a ‘chair’ conformation (Fig. 9c).

The molecular structures of the series of compounds examined in the course of this study are shown in Table 1. There is a clear movement from the ‘classic’ icosahedral  $C_{3v}$  structure to the *nido*-capped icosahedral form ( $C_s$ ). It is also apparent that there is a direct relationship between the size of the metal core (average) and the polyhedral form adopted by the ligand shell. Ideally, the icosahedron (I) is adopted since it optimises ligand–ligand interactions. However, as the metal core size increases, a steric strain is created within the icosahedron. The upper limit is observed in  $[\text{Rh}_4(\text{CO})_{12}]$ , where a more accurate structural re-determination revealed a deviation of the cluster from a  $C_{3v}$  geometry towards a  $C_s$  geometry (Fig. 10) [9].

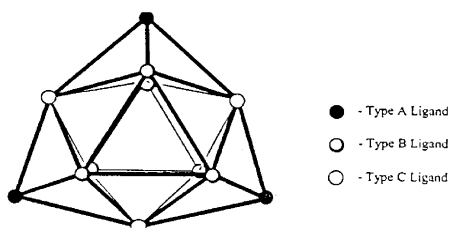


Fig. 7. The three types of ligand environments in the  $D_{3h}$  icosahedron.

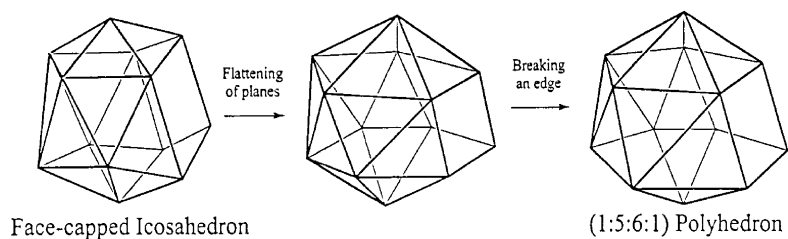
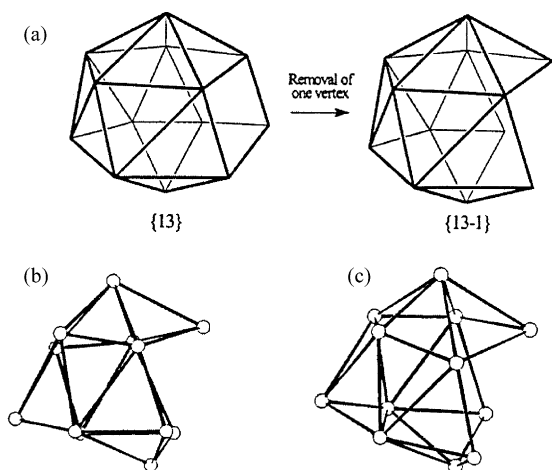


Fig. 8. The formation of the (1:5:6:1) polyhedron from the face-capped icosahedron.

Fig. 9. Comparison between the *nido*-(1:5:6:1) polyhedron and the distorted icosahedral ligand polytope of  $[\text{Rh}_3\text{Ru}(\text{CO})_{12}]^-$ ,  $[\text{Rh}_3\text{Os}(\text{CO})_{12}]^-$  and  $[\text{Rh}_2\text{Ru}_2(\text{CO})_{12}]^{2-}$ .

Here, two *pseudo*-equatorial carbonyls, CO(7) and CO(11), are tilted further out of the basal plane defined by Rh(2)–Rh(3)–Rh(4) than the carbonyl CO(9). The distances of the atoms O(7), O(9) and O(11) from this basal plane are 1.434(4), 1.108(6) and 1.772(3) Å, re-

spectively. The ligand polytope also deviates slightly from an icosahedron, with one edge broken (Fig. 10). This may be viewed as approaching a {13–1} polyhedron.

The dianionic cluster  $[\text{Ru}_3\text{Ni}(\text{CO})_{12}]^{2-}$  may be considered as an intermediate in the distortion process towards the *nido*-(1:5:6:1) polyhedral form (Fig. 11). This cluster possesses four bridging carbonyls (one bridging the basal and apical metal atoms) and the structure lies between that of clusters with three bridging carbonyls ( $C_{3v}$  structure) and those with five bridging carbonyls ( $C_s$  structure) in a structural continuum. The ligand polytopes can be described as a distorted icosahedron, with two edges broken (Fig. 11).

At the bottom of Table 1, the three clusters of  $[\text{Rh}_3\text{Ru}(\text{CO})_{12}]^-$ ,  $[\text{Rh}_3\text{Os}(\text{CO})_{12}]^-$  and  $[\text{Rh}_2\text{Ru}_2(\text{CO})_{12}]^{2-}$  possess the largest metal cores (2.81–2.82 Å) [2–4]. Here, the average metal–metal bond length is at least 0.1 Å longer than those found in  $[\text{Rh}_4(\text{CO})_{12}]$ . As a result, further distortions are observed and the ligand polytope deviates from the icosahedron by the breaking of more edges. These clusters possess a  $C_s$  geometry, with two of the equatorial carbonyls tilted so far away from the basal metal plane that they adopt a semi-bridging bonding mode (Fig. 12).

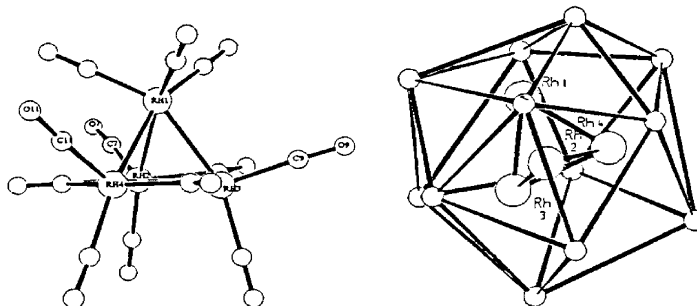
Fig. 10. The local bonding scheme of  $[\text{Rh}_4(\text{CO})_{12}]$  and its LMP representation.

Table 1  
Carbonyl polyhedra as a function of core size

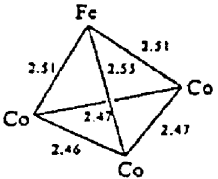
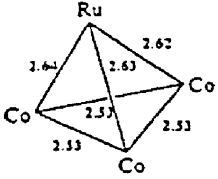
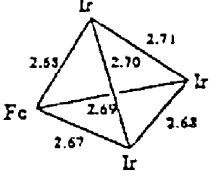
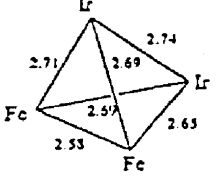
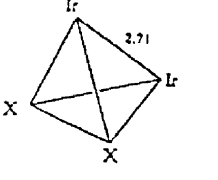
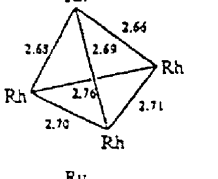
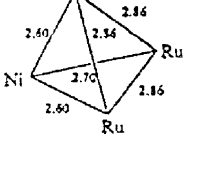
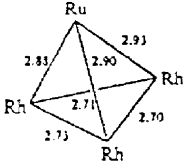
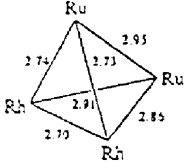
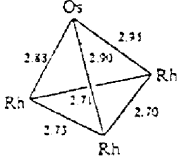
Cluster	M–M bond lengths (Å)	Average M–M bond lengths (Å)	Ligand shell geometry	Reference
$[\text{Co}_3\text{Fe}(\text{CO})_{12}]^-$		2.50	Icosahedron ( $C_{3v}$ )	[15]
$[\text{Co}_3\text{Ru}(\text{CO})_{12}]^-$		2.58	Icosahedron ( $C_{3v}$ )	[11]
$[\text{Ir}_3\text{Fe}(\text{CO})_{12}]^-$		2.69	Icosahedron ( $C_{3v}$ )	[13]
$[\text{Ir}_2\text{Fe}_2(\text{CO})_{12}]^{2-}$		2.68	Icosahedron ( $C_{3v}$ )	[13]
$[\text{Ir}_3\text{Ru}(\text{CO})_{12}]^-$ (X: Ru/Ir)*		$\sim 2.71^*$	Icosahedron	[14]
$[\text{Rh}_4(\text{CO})_{12}]$		2.70	Icosahedron (one edge broken)	[9]
$[\text{Ru}_3\text{Ni}(\text{CO})_{12}]^{2-}$		2.75	Slightly distorted icosahedron (two edges broken)	[16]

Table 1 (Continued)

Cluster	M–M bond lengths (Å)	Average M–M bond lengths (Å)	Ligand shell geometry	Reference
$[\text{Rh}_3\text{Ru}(\text{CO})_{12}]^-$		2.81	Highly distorted icosahedron (four edges broken) ( $C_3$ )	[2]
$[\text{Rh}_2\text{Ru}_2(\text{CO})_{12}]^{2-}$		2.82	Highly distorted icosahedron (four edges broken) ( $C_3$ )	[3]
$[\text{Rh}_3\text{Os}(\text{CO})_{12}]^-$		2.81	Highly distorted icosahedron (four edges broken) ( $C_3$ )	[4]

\* Disorder in the  $[\text{Ir}_3\text{Ru}(\text{CO})_{12}]^-$  crystal prevents an accurate measurement of the M–M bond lengths.

This distortion pathway away from the ideal icosahedron is very similar to that found for five-coordinate molecules, where a continuum of structures, e.g.  $[\text{CdCl}_5]^{3-}$ , gradually distorts from the ideal trigonal bipyramid towards the square pyramid, e.g.  $[\text{Cd}(\text{C}_6\text{H}_7\text{NO})_5]^{2+}$  and  $[(\text{C}_6\text{H}_5)_5\text{Sb}]$ , and finally to the ideal square pyramidal geometry found in  $[\text{Ni}(\text{CN})_5]^{3-}$  (see above) [12]. In Fig. 13, the structural variation, parallels that of the five-coordinate molecule. It is clear that it represents a continuum of structures undergoing distortion from the {12} to a {13–1} polyhedron.

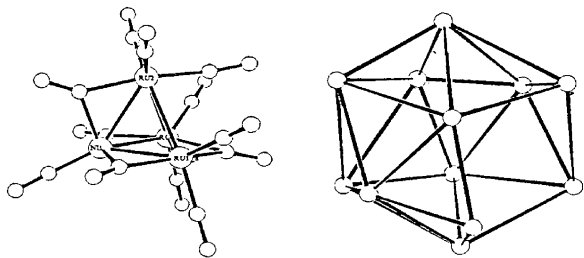


Fig. 11. The local bonding scheme of  $[\text{Ru}_3\text{Ni}(\text{CO})_{12}]^{2-}$  and its ligand polytope.

The reasons for these distortions are complex and at the moment not fully understood. From Table 1, it would appear that the distortion in the ligand shell may be rationalised in terms of a movement of the ligands to accommodate the larger metal core. The final polyhedron resembles that of a 13-vertex polyhedron {13–1} because of the greater ability of this larger polyhedron to accommodate a larger metal core (2.72–2.81 Å) (Table 1) than the icosahedron (2.50–2.70 Å) (Table 1). These higher values are of the order of the metal core sizes found in

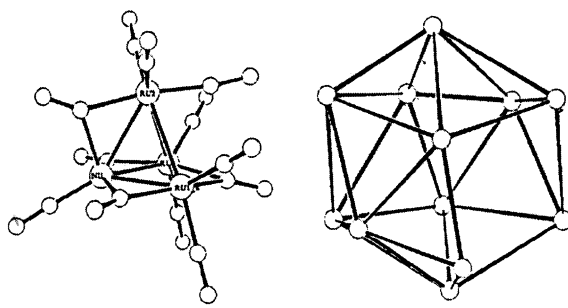


Fig. 12. The local bonding scheme of  $[\text{Rh}_3\text{Ru}(\text{CO})_{12}]^-$ ,  $[\text{Rh}_2\text{Ru}_2(\text{CO})_{12}]^{2-}$  and  $[\text{Rh}_3\text{Os}(\text{CO})_{12}]^-$ , and their ligand polytope.

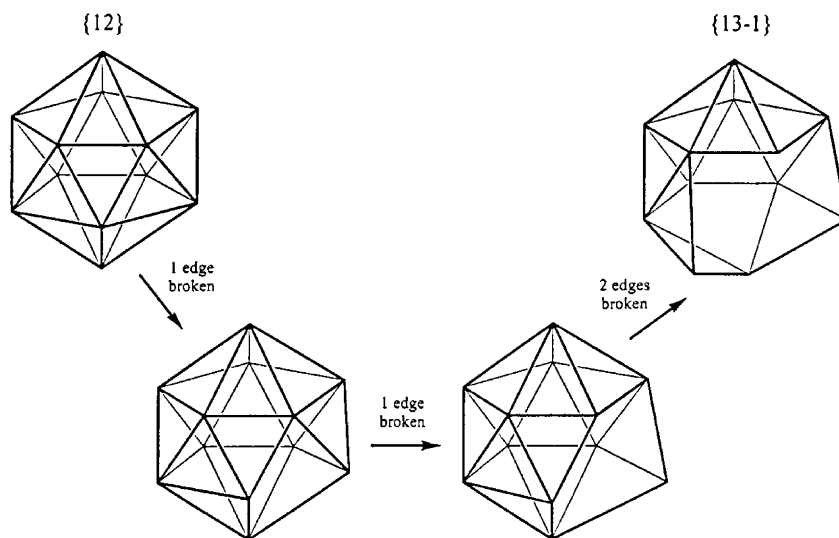


Fig. 13. Proposed distortion mode of the icosahedron to *nido*-(13-vertex polyhedron).

$[\text{Rh}_3\text{Ru}(\text{CO})_{12}]^-$  (2.81 Å),  $[\text{Rh}_3\text{Os}(\text{CO})_{12}]^-$  (2.81 Å) and  $[\text{Rh}_2\text{Ru}_2(\text{CO})_{12}]^{2-}$  (2.82 Å). Hence, we can conclude that size and hence steric factor play a major role in the determination of carbonyl cluster structures.

However, the reason why  $[\text{Rh}_4(\text{CO})_{12}]$  should adopt a structure significantly different to that of  $[\text{Ir}_4(\text{CO})_{12}]$  with the CO shell is difficult to understand. It must be said that the cleavage of one edge in the carbonyl polyhedron for  $[\text{Rh}_4(\text{CO})_{12}]$  is understandable and follows ‘naturally’ from the size increase of the  $\text{Rh}_4$  unit from the  $\text{Co}_4$  unit but the substantial change in structure in going to the cubeoctahedral  $[\text{Ir}_4(\text{CO})_{12}]$  is more difficult to appreciate. As with  $[\text{Fe}_3(\text{CO})_{12}]$  and  $[\text{Os}_3(\text{CO})_{12}]$  this difference may arise from the greatly increased stability of the metal–metal bond and the need to provide good metal orbital–metal orbital overlap dictates the final structure. Similarly, the adoption of the *nido*- $D_{3h}$  icosahedral ligand polytope in  $[\text{Rh}_4(\text{CO})_{11}]^{2-}$  is difficult to understand. It may be attributed to the very high bridging-to-terminal ratio of carbonyl ligands that results. The higher  $\pi$ -acidity of the bridging carbonyl ligands promotes interaction with the filled d orbitals of the rhodium atoms, allowing for greater charge distribution within this dianionic cluster. As seen in Fig. 6, the structure possesses seven bridging carbonyls and four terminal carbonyls. Thus, the observed ligand stereochemistry can be regarded as a compromise between both steric and electronic

requirements which becomes more relevant in the shift from neutral to anionic species. However, in our view, the most important steric factors are the optimisation of inter-ligand interactions (i.e. adoption of the most stable polyhedron) and accommodation of the metal core. For electronic factors, a good overall charge distribution (especially for anionic clusters) and reasonable local electron book-keeping on all the metal centres are important.

### 3. Conclusion

In conclusion, this paper reaffirms the ability of the LPM to rationalise cluster structures in terms of one polyhedron (the metal) within another (the carbonyl). Although only a few examples of *nido*-polyhedra have been shown so far, further investigations should reveal more such examples in other polyhedral geometries e.g.  $\{7-1\}$ ,  $\{8-1\}$ ,  $\{9-1\}$ , etc. Although many factors are known to be involved in determining cluster structures, we have shown here that steric factors remain dominant. Hence, the LPM, which is based mainly on steric interactions, continues to be a useful tool in the rationalisation of cluster structures. However, it is clear that the introduction of anionic charge or possibly the presence of the counter cation(s) influence the final carbonyl ligand arrangement.



## References

- [1] B.F.G. Johnson, R.E. Benfield, *J. Chem. Soc., Dalton Trans.* (1978) 1554.
- [2] A. Fumagalli, M. Bianchi, M.C. Malatesta, G. Ciani, M. Moret, A. Sironi, *Inorg. Chem.* 37 (1998) 1324.
- [3] A. Fumagalli, D. Italia, M.C. Malatesta, G. Ciani, M. Moret, A. Sironi, *Inorg. Chem.* 35 (1996) 1765.
- [4] A. Fumagalli, S. Martinengo, G. Ciani, M. Moret, A. Sironi, *Inorg. Chem.* 31 (1992) 2900.
- [5] B.F.G. Johnson, *Inorg. Chem. Acta* (1992) 447.
- [6] F.Y. Lo, G. Longoni, P. Chini, L.D. Lower, L.F. Dahl, *J. Am. Chem. Soc.* 102 (1980) 7691.
- [7] J. Liu, E.P. Boyd, S.G. Shore, *Acta Crystallogr. A* 55 (1999) 29.
- [8] C.C. Nagel, J.C. Bricker, D.G. Always, S.G. Shore, *J. Organomet. Chem.* 219 (1981) C9.
- [9] L.J. Farrugia, *J. Cluster Sci.* 11 (2000) 39.
- [10] V.G. Albano, G. Ciani, A. Fumagalli, S. Martinengo, W.M. Anker, *J. Organomet. Chem.* 116 (1976) 343.
- [11] M. Hidai, M. Orisaku, M. Ue, Y. Koyasu, T. Kodama, Y. Uchida, *Organometallics* 2 (1983) 292.
- [12] E.L. Muetterties, L.J. Guggenberger, *J. Am. Chem. Soc.* 96 (1974) 1748.
- [13] R.D. Pergola, L. Garlaschelli, F. Demartin, M. Manassero, N. Masciochi, M. Sansoni, *J. Chem. Soc., Dalton Trans.* (1990) 127.
- [14] A. Fumagalli, F. Demartin, A. Sironi, *J. Organomet. Chem.* 279 (1985) C33.
- [15] B. Wu, Q. Suo, R. Wu, Q. Lu, Y. Wang, J. Chen, X. Huang, *Chin. Struct. Chem.* 17 (1998) 101.
- [16] E. Brivio, A. Ceriotti, R.D. Pergola, L. Garlaschelli, M. Manassero, M. Sansoni, *J. Cluster Sci.* 6 (1995) 27.